Design of a direct control strategy for a static shunt compensator to improve power quality in polluted and unbalanced grids

Antoine F. Hanna Nohra, Maurice Fadel, Hadi Y. Kanaan

Design of a direct control strategy for a static shunt compensator to improve power quality in polluted and unbalanced grids

Antoine F. Hanna Nohra[1,2,3], Maurice Fadel[1,2] and Hadi Y. Kanaan[3]

[1] Université de Toulouse ; INPT, UPS ; ENSEEIHT, 2 rue Charles Camichel, BP 7122, Toulouse, France
[2] CNRS; LAPLACE; F-31071 Toulouse, France
[3] Saint-Joseph University of Beirut, Faculty of Engineering – ESIB, Mar Roukoz, Mkalles, B.P. 11-0514, Beirut, Lebanon
antoine.hannanohra@laplace.univ-tlse.fr , maurice.fadel@laplace.univ-tlse.fr ,

***Abstract* – Many control techniques for three-phase active filters with the aim of improving the power factor and reducing the current harmonic distortion at the source level exist today and are widely reported in the scientific literature. Almost all of these methods are designed for a perfect sine-wave source and don't perform sinusoidal current when voltages are distorted or unbalanced. The work developed in this paper concerns the active filtering on a perturbed and unbalanced network. First, the proposed control method is described and validated by simulations and experimental results, and then the proposed method is compared to the classical control laws such as the original p-q theory, the modified p-q theory and the p-q-r method. Experimental results are conducted on a three-wire low power distribution network under perturbed voltage and non-linear load using a DSPACE control system. The assessment is performed on the source currents after filtering, and a comparative evaluation in terms of unbalance factor and current Total Harmonic Distortion (THD_i) is carried out for all methods.**

***Keywords* – Active filter, voltage disturbance, voltage unbalance, three-phase power grid, harmonic distortion, unbalance factor, direct power control, instantaneous power control**

1. Introduction

The increase of the non-linear loads connected to distributed electric power networks leads to an excessive injection of harmonics and the circulation of reactive power in the distribution lines. These periodic but non-sinusoidal currents circulate through the impedances of the grid and give rise to non-sinusoidal voltages that are added to the initial voltage [1]. Consequently, the

degradation of the power quality [2] has detrimental consequences on the proper functioning of electrical appliances and incurs an additional cost for the installations. This causes severe damages that must be fought forcefully [3]. The ability of shunt active filters to remove these problems has given rise to a great deal of work in recent years and many solutions have emerged. Most of these solutions are based on the concept of instantaneous reactive power and on the *p-q* theory. This approach is particularly effective but is based on the assumption of purely sine-wave source voltages. If the voltage source is distorted, both power factor and efficiency are reduced. In this paper, the development of a novel method called Direct Control for Active Power (DCAP) based on the concept of instantaneous active power and on the computation of the effective value of the fundamental of the source voltages is proposed. A new definition of desired active current under perturbed and unbalanced supply voltages is developed. It is based on the active power to be delivered by the source and the fundamental of perturbed voltages obtained by a Band-pass filter rather than a PLL. The PLL extract the direct-sequence voltages system but the DCAP method explicitly takes into account the unbalance of voltages in the calculation of reference currents. PLL is commonly used in the control of SAPF [4-6] in particularly associated to the D-Q theory [7-11]. Several works investigated on the output response of a PLL under distorted and unbalanced utility voltages and demonstrated that a PLL cannot perform at its output sinusoidal waves in disturbed environment [6]. Indeed, some of its components require fine adjustments taking into account numerous parameters [12].

The DCAP method takes part of a general methodology applicable in multiphase systems particularly in three phase 3-wire, three-phase 4-wire and in single phase networks. The general approach for polyphase system described in [13], has been the subject of a patent application [14].

This paper is divided as follow: In section 2, the Active Power Filter APF and its control scheme are described. In section 3, control strategies based on the p-q theory, modified p-q theory, and p-q-r method are presented; the proposed DCAP method is also detailed. In section 4, the application of the DCAP control on the three-phase shunt active power filter is studied; the setup procedure to generate a perturbed voltage source (with THD = 25%) is described, and the simulation and experimental results are analysed and discussed through comparative evaluation of all considered control methods. This work finally ends with some conclusions.

2. Shunt active power filter: Topology and control scheme

The shunt active power filter (SAPF) is the most common solution for the cancellation of current-type harmonics [15-17]. The conventional structure of the two-level inverter shown in Fig. 1 is highly widespread for Low Voltage applications. Fig. 2 shows the general control scheme applied to one phase, e.g. phase (a). It reveals 3 essential functions, first a block to extract the harmonics and reactive current $i_{r,h}$ to be compensated, a current loop and a voltage loop.

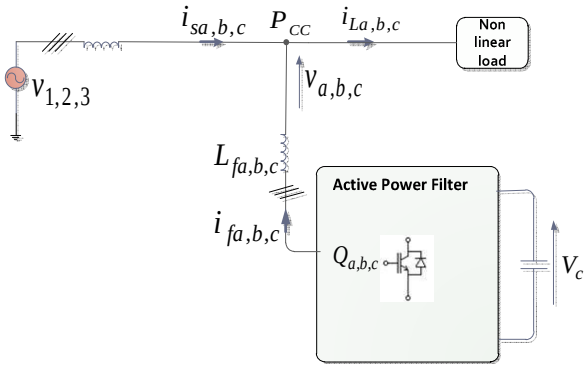

Fig.1. Three-wire grid connected Active Power Filter

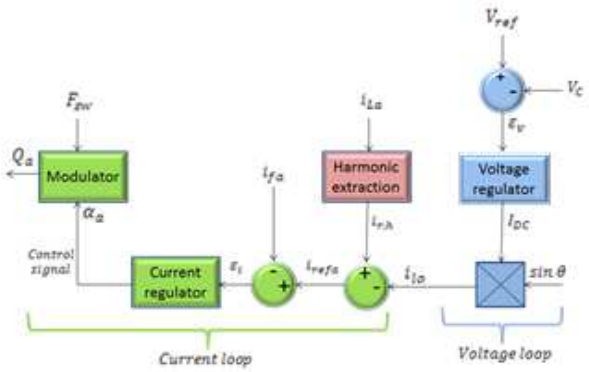

Fig. 2. General control scheme of the SAPF law

The proposed work mainly focuses on the design of harmonic extraction block. This block in its simplest version uses only the load current as input but it would be possible to use the power instead as it will be explained in the proposed control method.

3. Control strategies for APF

3.1 P-Q theory in three-phase systems

The p-q theory, initially developed for the three-phase systems by Akagi and al. [18], is one of the theories more appropriate to generate current references in current controlled systems [19-23]. It is characterized by a high dynamic response and stable steady-state, and is based on a transformation of currents and voltages vectors from the a,b,c to the α,β frame as in equations (1) and (2). The instantaneous active power *p(t)* and an instantaneous reactive power *q(t)* are defined expressed in (4), where $\boldsymbol{C}_{23}$ is the Concordia matrix in (3).

$$\begin{bmatrix} i_\alpha \\ i_\beta \end{bmatrix} = \boldsymbol{C}_{23} \cdot \begin{bmatrix} i_a \\ i_b \\ i_c \end{bmatrix} \tag{1}$$

$$\begin{bmatrix} v_\alpha \\ v_\beta \end{bmatrix} = \boldsymbol{C}_{23} \cdot \begin{bmatrix} v_a \\ v_b \\ v_c \end{bmatrix} \tag{2}$$

$$\boldsymbol{C}_{23} = \sqrt{\frac{2}{3}} \cdot \begin{bmatrix} 1 & -1/2 & -1/2 \\ 0 & \sqrt{3}/2 & -\sqrt{3}/2 \end{bmatrix} \tag{3}$$

$$\begin{bmatrix} p \\ q \end{bmatrix} = \begin{bmatrix} v_\alpha & v_\beta \\ -v_\beta & v_\alpha \end{bmatrix} \cdot \begin{bmatrix} i_\alpha \\ i_\beta \end{bmatrix} \tag{4}$$

The currents to be generated by the SAPF are given in (5) and obtained by the inversion of (4):

$$\begin{bmatrix} i_{r\alpha} \\ i_{r\beta} \end{bmatrix} = \frac{1}{v_\alpha^2 + v_\beta^2} \begin{bmatrix} v_\alpha & -v_\beta \\ v_\beta & v_\alpha \end{bmatrix} \cdot \begin{bmatrix} p_C \\ q_C \end{bmatrix} \tag{5}$$

To perform compensation without using energy storage component it is good enough to eliminate the instantaneous reactive power without altering the active power like as (6).

$$\begin{cases} q_C = \bar{q} + \tilde{q} \\ p_C = 0 \end{cases} \tag{6}$$

To eliminate harmonics and reactive power, the undesirable powers to be compensated are expressed in (7):

$$\begin{cases} q_C = \bar{q} + \tilde{q} \\ p_C = \tilde{p} \end{cases} \tag{7}$$

Finally, the current references obtained in α, β frame, which take into account the losses in the filter and the power p_f requested for the DC bus voltage regulation, are formulated in (8):

$$\begin{bmatrix} i_{r\alpha} \\ i_{r\beta} \end{bmatrix} = \frac{1}{v_\alpha^2 + v_\beta^2} \begin{bmatrix} v_\alpha & -v_\beta \\ v_\beta & v_\alpha \end{bmatrix} \cdot \begin{bmatrix} \tilde{p} - p_f \\ \bar{q} + \tilde{q} \end{bmatrix} \tag{8}$$

The bloc diagram in Fig. 3 shows the steps to extract the reference currents on the a, b, c frame.

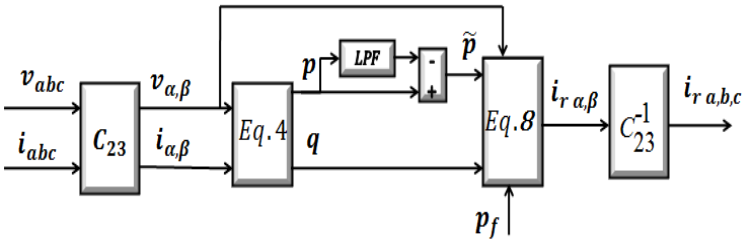

Fig. 3. Bloc diagram to extract the current references based on the p-q theory

The p_f power reference is provided by the voltage loop allowinga quasi-constant voltage Vc across the capacitor. The LPF filter that separates the DC and AC components is set at a few hertz.

3.2 Modified P-Q theory in three phase

The modified p-q theory [24,25] is based on the definition of three reactive powers and an active power, and it is dedicated in priority for 4-wire systems and formulated in (9).

$$\begin{bmatrix} p \\ q_0 \\ q_\alpha \\ q_\beta \end{bmatrix} = \begin{bmatrix} v_0 & v_\alpha & v_\beta \\ 0 & -v_\beta & v_\alpha \\ v_\beta & 0 & -v_0 \\ -v_\alpha & v_0 & 0 \end{bmatrix} \cdot \begin{bmatrix} i_0 \\ i_\alpha \\ i_\beta \end{bmatrix} \tag{9}$$

Its application in 3-wire systems is a particular case from (9) for $i_0 = 0$. In this paper, the application aims the active filtering on a perturbed 3-wire network. Accordingly, $v_0 \neq 0$ and $i_0 = 0$.

It is then possible to eliminate the first column in (9), and the reference currents are thus obtained by the inversion of (9) and are formulated in (10):

$$\begin{bmatrix} i_{r\alpha} \\ i_{r\beta} \end{bmatrix} = \frac{1}{v_{0\alpha\beta}^2} \cdot \begin{bmatrix} v_\alpha & -v_\beta & 0 & v_0 \\ v_\beta & v_\alpha & -v_0 & 0 \end{bmatrix} \cdot \begin{bmatrix} p_C \\ q_{0C} \\ q_{\alpha C} \\ q_{\beta C} \end{bmatrix} \tag{10}$$

With:

$$v_{0\alpha\beta} = \sqrt{v_0^2 + v_\alpha^2 + v_\beta^2} \tag{10.a}$$

To compensate harmonics and reactive power, the reference compensation powers are:

$$\begin{cases} p_C = \tilde{p} \\ q_{C0} = q_0 \\ q_{C\alpha} = q_\alpha \\ q_{C\beta} = q_\beta \end{cases} \tag{11}$$

The system of reference currents obtained in α, β frame is consequently formulated as:

$$\begin{bmatrix} i_{r\alpha} \\ i_{r\beta} \end{bmatrix} = \frac{1}{v_{0\alpha\beta}^2} \begin{bmatrix} v_\alpha & -v_\beta & 0 & v_0 \\ v_\beta & v_\alpha & -v_0 & 0 \end{bmatrix} \begin{bmatrix} \tilde{p} - p_f \\ q_0 \\ q_\alpha \\ q_\beta \end{bmatrix} \tag{12}$$

The block diagram in Fig. 4 shows the extraction of reference currents on the a, b, c frame.

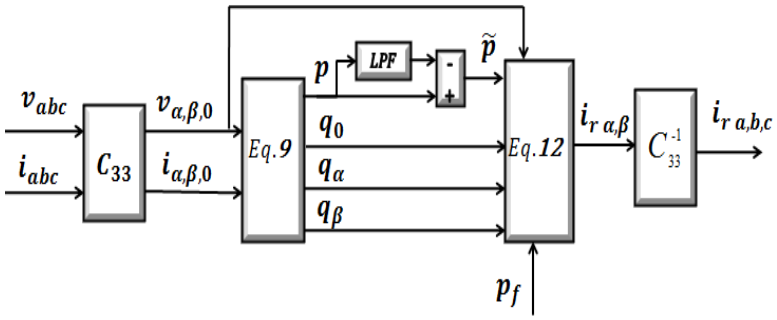

Fig. 4. Bloc diagram to extract the reference currents based on the modified p-q theory

3.3 P-Q-R theory in three phase

For this method [26-31], two transformations are required. Once the currents are calculated in the $\alpha, \beta, 0$ frame, another transformation to the p, q, r frame is necessary (12). The pqr-coordinate is developed as well as space-vector transformation by using Euler rotation angle. By using the Euler angle method with double rotation, the mapping matrices model results in (12):

$$\begin{bmatrix} i_p \\ i_q \\ i_r \end{bmatrix} = \boldsymbol{T}_{pqr} \begin{bmatrix} i_0 \\ i_\alpha \\ i_\beta \end{bmatrix} \tag{12}$$

with:

$$\boldsymbol{T}_{pqr} = \frac{1}{v_{0\alpha\beta}} \cdot \begin{bmatrix} v_0 & v_\alpha & v_\beta \\ 0 & -\frac{v_{0\alpha\beta} \cdot v_\beta}{v_{\alpha\beta}} & \frac{v_{0\alpha\beta} \cdot v_\alpha}{v_{\alpha\beta}} \\ v_{\alpha\beta} & -\frac{v_0 \cdot v_\alpha}{v_{\alpha\beta}} & -\frac{v_0 \cdot v_\beta}{v_{\alpha\beta}} \end{bmatrix} \tag{13}$$

And:

$$v_{\alpha\beta} = \sqrt{v_\alpha^2 + v_\beta^2} \tag{13.a}$$

Note that, in the case of 3-wire system, the zero-sequence component of the phase currents is zero, i.e. $i_0 = 0$, but all equations remain valid and it is not necessary to reduce their expression. Automatically, all components that depend on i_0 become also zero. This methode is based on the difinition of an active power and two reactive powers as in (14):

$$\begin{bmatrix} p \\ q_q \\ q_r \end{bmatrix} = \begin{bmatrix} v_p . i_p \\ -v_p . i_r \\ v_p . i_q \end{bmatrix} = v_p . \begin{bmatrix} i_p \\ -i_r \\ . i_q \end{bmatrix} \tag{14}$$

In the p-q-r coordinate transformation two consecutive transformations are operated, the purpose of which is to cancel the voltage components on the q-axis and r-axis. So only one voltage is calculated on the p-axis that gives:

$$v_p = v_{0\alpha\beta} \tag{14.a}$$

There are two ways for the compensation in this method. The first is based on power compensation, which results are similar to those of the p-q and p-q modified methods. The second is based on the current compensation presented in the following.

The reference currents of the p, q, r frame are then in (15) and recalculated in the $\alpha, \beta, 0$ frame in (16)

$$\begin{cases} i_{r\,p} = \tilde{\imath}_p \\ i_{rq} = i_q \\ i_{rr} = i_r + \frac{i_p . v_0}{v_{\alpha\beta}} \end{cases} \tag{15}$$

$$\begin{bmatrix} i_{r\,0} \\ i_{r\alpha} \\ i_{r\beta} \end{bmatrix} = \boldsymbol{T}_{pqr}^{-1} \begin{bmatrix} i_{rp} \\ i_{rq} \\ i_{rr} \end{bmatrix} \tag{16}$$

$\boldsymbol{T}_{pqr}^{-1}$ is the inverse matrix of $\boldsymbol{T}_{pqr}$ expressed in (16.a).

$$\boldsymbol{T}_{pqr}^{-1} = \frac{1}{v_{0\alpha\beta}} . \begin{bmatrix} v_0 & 0 & v_{\alpha\beta} \\ v_\alpha & -\frac{v_{0\alpha\beta} . v_\beta}{v_{\alpha\beta}} & -\frac{v_0 . v_\alpha}{v_{\alpha\beta}} \\ v_\beta & \frac{v_{0\alpha\beta} . v_\alpha}{v_{\alpha\beta}} & -\frac{v_0 . v_\beta}{v_{\alpha\beta}} \end{bmatrix} . \begin{bmatrix} i_{rp} \\ i_{rq} \\ i_{rr} \end{bmatrix} \tag{16.a}$$

The block diagram in Fig. 5 shows the extraction of reference currents on the a, b, c frame.

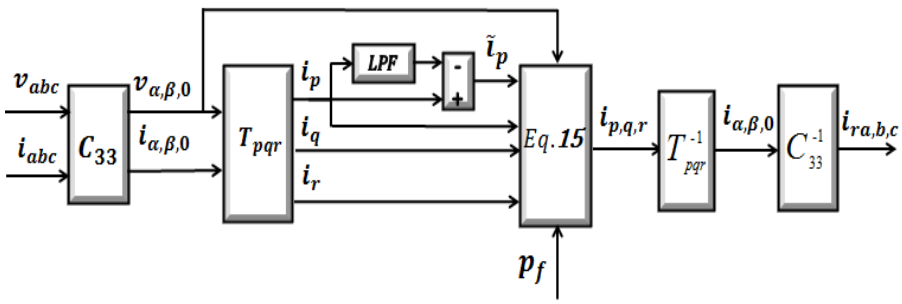

Fig.5. Bloc diagram to extract the reference currents based on the modified p-q-r theory.

3.4 DCAP theory in three phase

The proposed DCAP patented method [13,14] is based on the repartition of sinusoidal and balanced currents in the source side and not on the repartition of equal powers in the source linesIt is developped for a polyphase system and it has been demonstrated that the fundamental conductance of each phase, for a perturbed *k*-phase is then expressed in (17).

$$\begin{cases} G_{f1} = \dfrac{P_s}{V_{f1}.\left(\sum_{j=1}^{k} V_{fj}\right)} \\ G_{f2} = \dfrac{P_s}{V_{f2}.\left(\sum_{j=1}^{k} V_{fj}\right)} \\ \vdots \\ G_{fk} = \dfrac{P_s}{V_{fk}.\left(\sum_{j=1}^{k} V_{fj}\right)} \end{cases} \tag{17}$$

Where V_{fi} represent the rms voltage value of each of the phases of the network obtained by filtering.

The three phase system is a particular case of (17) for *k=3* and the desired currents in the source side $i_{sd\ a,b,c}$ for a 3 phase system are formulated as follows:

$$\begin{cases} i_{sda} = \dfrac{P_s}{V_{fa}.(V_{fa}+V_{fb}+V_{fc})}.v_{fa} \\ i_{sdb} = \dfrac{P_s}{V_{fb}.(V_{fa}+V_{fb}+V_{fc})}.v_{fb} \\ i_{sdc} = \dfrac{P_s}{V_{fc}.(V_{fa}+V_{fb}+V_{fc})}.v_{fc} \end{cases} \tag{18}$$

Where V_f represents the fundamental voltage of the network. So, the RMS value for desired equal currents is:

$$I_{sda} = I_{sdb} = I_{sdc} = \frac{P_s}{(V_{fa}+V_{fb}+V_{fc})} \tag{19}$$

Once the sinusoidal active currents desired in the source $i_{sd\ a,b,c}$ are calculated, the reference currents are deduced:

$$i_{r\,i} = i_{L\,i} - i_{sd\,i} \quad i = a, b, c. \tag{20}$$

P_s is the active power to be feeded by the source and deduced from:

$$P_s = P_L + P_f \tag{21}$$

P_L is the active power required by the load and obtained at the output of a Low Pass Filter after the calculation of the instantaneous power:

$$p_L(t) = v_a.i_{La} + v_b.i_{Lb} + v_c.i_{Lc} \tag{22}$$

P_f is the power to be absorbed by the filter and needed for the regulation of the DC bus voltage. It is expressed as:

$$P_f = I_{lo}.(V_{fa} + V_{fb} + V_{fc}) \tag{23}$$

I_{lo} is the RMS value of the required sinusoidal currents $i_{lo\ abc}$ that are calculated by the same way of (18) and formulated in (24).

$$\begin{cases} i_{lo\ a} = \frac{P_f}{V_{fa}.(V_{fa}+V_{fb}+V_{fc})}.v_{fa} \\ i_{lo\ b} = \frac{P_f}{V_{fb}.(V_{fa}+V_{fb}+V_{fc})}.v_{fb} \\ i_{lo\ c} = \frac{P_f}{V_{fc}.(V_{fa}+V_{fb}+V_{fc})}.v_{fc} \end{cases} \tag{24}$$

The block diagram for reference current extraction is in Fig.6. The fundamental waves v_{fabc} are obtained at the output of a band-pass filter (BPF) tuned on the fundamental frequency. Afterward, the squared fundamental voltages are filtered with a low pass filter (LPF) generating thus the RMS value V_{fabc} of fundamental voltage according to the following definition where T is the period of network voltage:

$$V_{fabc} = \frac{1}{T}\sqrt{\int_0^T v_{fabc}^2.d\theta} \tag{25}$$

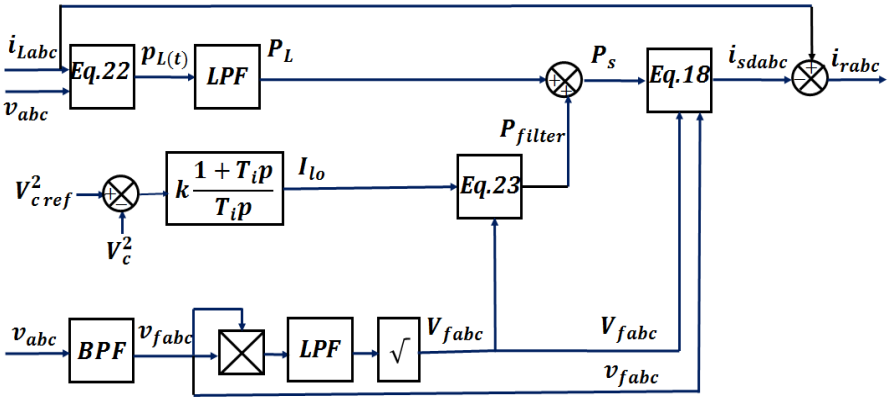

Fig.6 Block diagram for reference current extraction. DCAP method.

Once the current references $i_{r\ abc}$ to be injected by the filter are extracted, a closed-loop is then designed for the real currents injected by the filter $i_{f\ abc}$. The current control loop is presented in Fig.7 with F_{sw} being the switching frequency and Q_{abc} the switching signal.

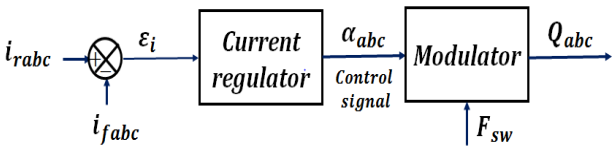

Fig.7. Bloc diagram for current loop

4. Application to three phase shunt active power filter control

Fig. 8 shows the studied three-phase shunt active power filter system configuration. It consists in a three-phase voltage source inverter, three series inductances L_{fabc} with internal resistances R_{fabc} and a DC capacitor. The shunt active power filter is connected in parallel to the non-linear load which is a three-phase diode rectifier feeding a (R_L, L_L) load. A R,L ac reactor is generally present at the input of this type of load.

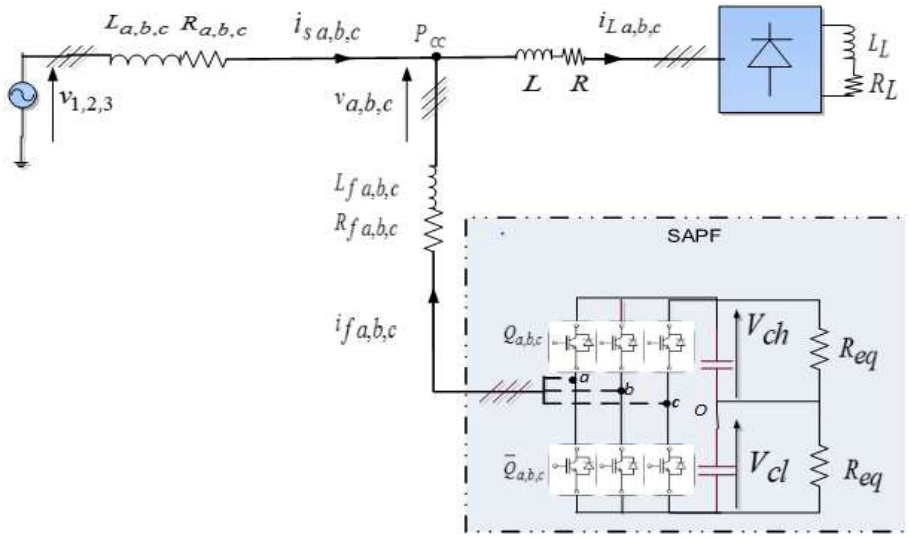

Fig.8. The three-phase three-wire power circuit.

v_1, v_2, and v_3 represent the voltages at the source (the output of transformer in the real case) with their harmonic expressions in (26). Three large unequal impedances $Z_{a,b,c}$ are connected between the source and the P_{CC}, (R_a=44.4 Ω, R_b= 35 Ω et R_c=38.3 Ω) in series with (L_a= 45 µH, L_b = 20 µH et L_c = 21 µH). The load is constituted by a three phase diode bridge that feed a resistance R_L=40.4Ω and an inductance L_L=27.67mH. Three identical impedances are connected at the ac input of the bridge L= 6,7 mH, R=0.5 Ω. The APF connected to the grid via three unequal inductances (L_{fa}=12.81mH, L_{fb}=13.72 mH and L_{fc}=10.6mH) in series with their internal resistances (R_{fa}= 0.5Ω, R_{fb}=0.6Ω and R_{fc}=0.3Ω). The DC bus voltage is 650V. The maximum voltage for each capacitor is 400V, for it they are two capacitors in series. C_h=C_b=0.6mF. The switching frequency is equal to 10 kHz.

4.1 Voltage perturbation procedure

4.1.a Simulation model

Simulation is performed using Psim tools. The power system parameters are identical to those in real experimentation. Harmonic model for measured real voltages source v_1, v_2, and v_3 are expressed like as (26) with numerical values for fundamentals and harmonic components in table.1 for *i* = 1,2,3.

$$v_i = \sum_{j=1;3;5;7;9;11} A_j . \sin(j . \omega . t - \varphi_j) \quad (26)$$

Table.1 Numerical values for voltages amplitudes A_j and harmonics phase shift φ_j .

	A_1	φ_1	A_3	φ_3	A_5	φ_5	A_7	φ_7	A_9	φ_9	A_{11}	φ_{11}
v_1	335.4	0	1.27	-43	7.77	171	3.39	-24	0.84	130	0.42	120
v_2	337.4	120	1.28	-2	7.9	53	2.54	104	1.41	138	0.42	-5
v_3	333.4	240	0.3	278	8	291	2.92	-216	0.84	158	0.14	212

On no load operation, voltages are initially slightly perturbed with values for THD respectively 2,6%, 2,5% and 2,5% and unbalanced with RMS values V_{1eff}=237.1V, V_{2eff}= 238.5V et V_{3eff}= 235.7V. When currents before filtering, in Fig.9, pass through the large impedances $Z_{a,b,c}$ having different values, it leads to large unequal voltages drops that induce unbalance on the voltages $v_{a,b,c}$ at the P_{CC} in Fig.10.

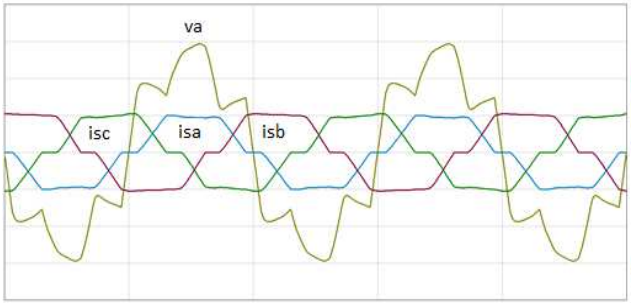

Fig.9. Source currents and v_a voltage before filtering obtained by simulated model (50V-5A-5ms/div)

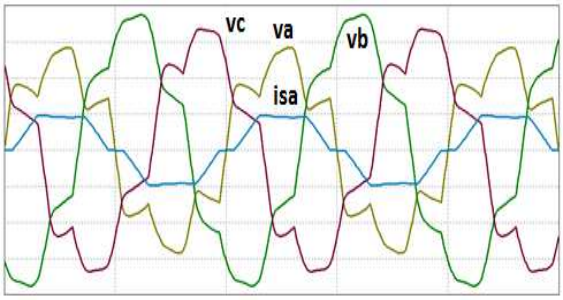

Fig.10. Voltages at P_{cc} and i_{sa} source current before filtering obtained by simulated model (50V-5A-5ms/div)

The RMS value V_f of the fundamental of each voltage decreases because of the voltage drop then the THD (27) increases for the same harmonic component V_h and voltages become highly perturbed see Table.2.

$$THD\% = \frac{\sqrt{\sum_{k=2}^{\infty} V_k^2}}{V_f} = \frac{V_h}{V_f} \quad (27)$$

4.1.b Experimental model

In figure 11.a below, we present the test bench which shows, in part A, the inverter with its control based on Dspace 1005 card of a DSPACE prototyping system associated with a FPGA card for the generation of the switching pattern. Next, the filter reactor in part B, afterwards the load in part C and the measurement and acquisition devices in part D. Results are recorded with Teledyne Lecroy (wavesurfer 3024, 200Mhz, 4Gs/s) oscilloscope and Fluke 438B device.

Figure.11.b illustrates the steps for experimental test. Voltages supply $v_{a,b,c}$ and load currents $i_{L\,a,b,c}$ are measured as analog inputs and data are transfered to the simulink model via the card DS2004 A/D converter and DS4003 I/O card dedicated for communication with DS1005 Dspace board for real-time calculation. The control algorithm of the active filter is then designed in Matlab/ Simulink and the control signals obtained at the output of the simulink model are transfered to the FPGA card also via DS4003 card. The PWM modulation is carried out by the FPGA card and the output magnitude is adapted to command the drivers

for IGBT semi-conductors. The regulation of current references and DC bus voltage is also performed in the simulink model compared with the real data of filter currents $i_{f\,a,b,c}$ and v_c feedback signals measured as analog inputs. The syncronization of voltages at the output of the filter and source voltages is automatically obtained because the control algorithm of the DCAP method generats reference currents synchronized with the fundamental of voltages extracted by a band-pass filter. İt is no need for a PLL for this method.

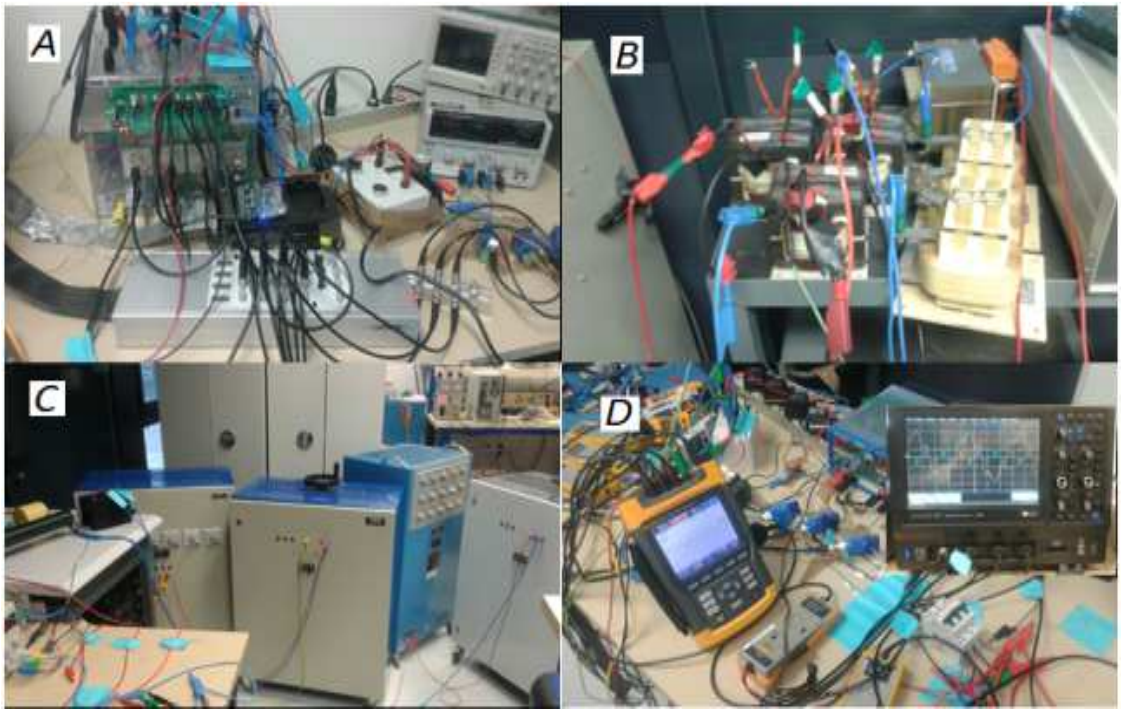

Fig.11.a Experimental test bench

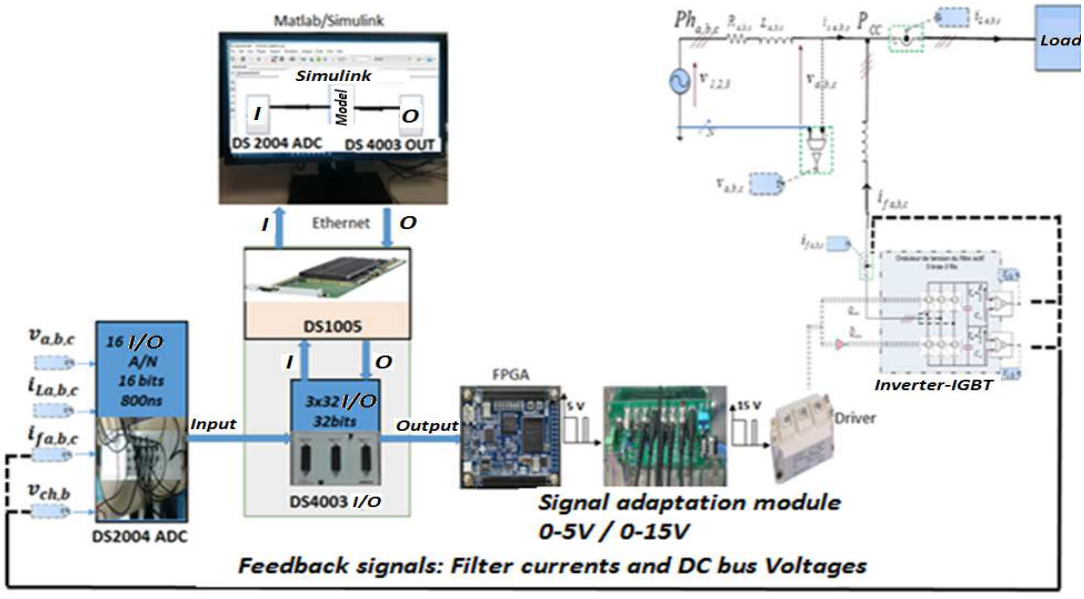

Fig.11.b Steps for experimental procedure.

Fig.12 shows results for polluted and unbalanced voltages at the P_{cc} before filtering. On its turn, the unbalanced voltage system induces unbalancing in currents system showing in Fig.13.

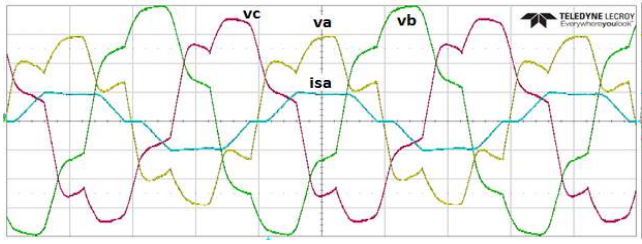

Fig.12. Experimental results before filtering for voltages at P_{cc} and i_{sa} source current (50V-5A-5ms/div).

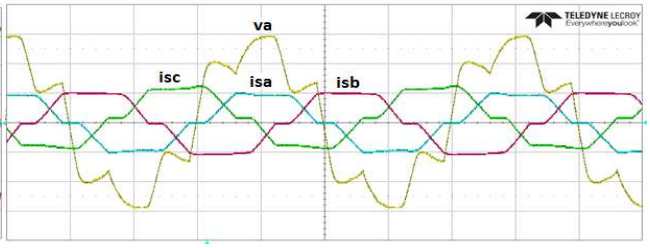

Fig. 13. Experimental results before filtering for source currents and v_a voltage (50V-5A-5ms/div)

Table.2 presents numerical values for unbalanced voltages source THD and RMS and Table.3 presents numerical values for unbalanced source current THD and current RMS for both experimental and simulated models before filtering.

Table.2: Numerical values of THD and voltages RMS before filtering obtained from experimental and simulated models

Voltages at Pcc		v_a	v_b	v_c
Experimental	*THD %*	*25.8*	*13.3*	*17.8*
Simulated	*THD %*	*25.4*	*13.3*	*17.7*
Experimental	*RMS (V)*	*79*	*108*	*96.5*
Simulated	*RMS (V)*	*79*	*106.4*	*95.3*

Table3: Numerical values of THD and currents RMS before filtering obtained from experimental and simulated models

Source currents		i_{sa}	i_{sb}	i_{sc}
Experimental	*THD %*	*14.2*	*12.9*	*14.1*
Simulated	*THD %*	*14.4*	*13.3*	*14*
Experimental	*RMS (V)*	*3.6*	*3.953*	*3.764*
Simulated	*RMS (V)*	*3.617*	*3.953*	*3.788*

The current unbalance factor *UF* before filtering is measured 4.9% on the diagram showing in Fig.14 according to the European standard EN 50160 based on $UF\% = \frac{Xi}{Xd}$ where Xd and Xi are the direct and inverse-sequence components of voltages. RMS values of source currents are also presented on this Fig.14. Measures are done with Fluke 438 device.

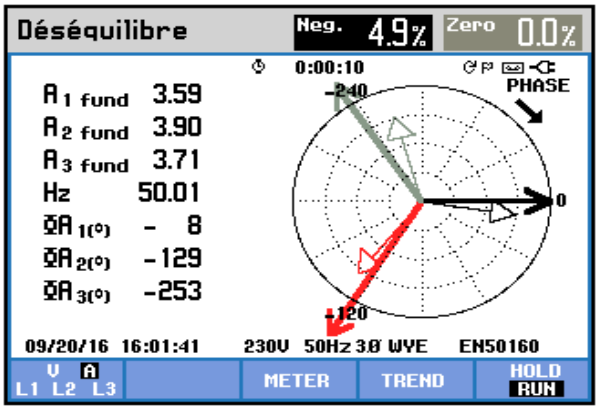

Fig.14. Current unbalance diagram before filtering

At this step of work it is shown that the simulated and experimental models before filtering ensure the same performances in terms of currents waveforms and numerical values for THD_i and RMS given in Table.2 and Table.3. Then, the effectiveness of simulated model under polluted and unbalanced supply voltages is demonstrated and that permit to conduct effective comparison after filtering between the different methods mentioned above.

4.2 Comparison of performances after filtering between DCAP and existing methods

Experimentation is carried out under perturbed supply voltages as shown in Fig.12 above. Fig. 15. shows the system of currents at the source referenced to the voltage v_a of the phase a. After filtering, the perturbation of voltages is reduced. Figure 15.a1, Fig.15.b1, Fig.15.c1 and Fig.15.d1 show the experimental results for the four methods after filtering compared with their associated simulation results in Fig.15.a2, Fig.15.b2, Fig.15.c2 and Fig.15.d2.

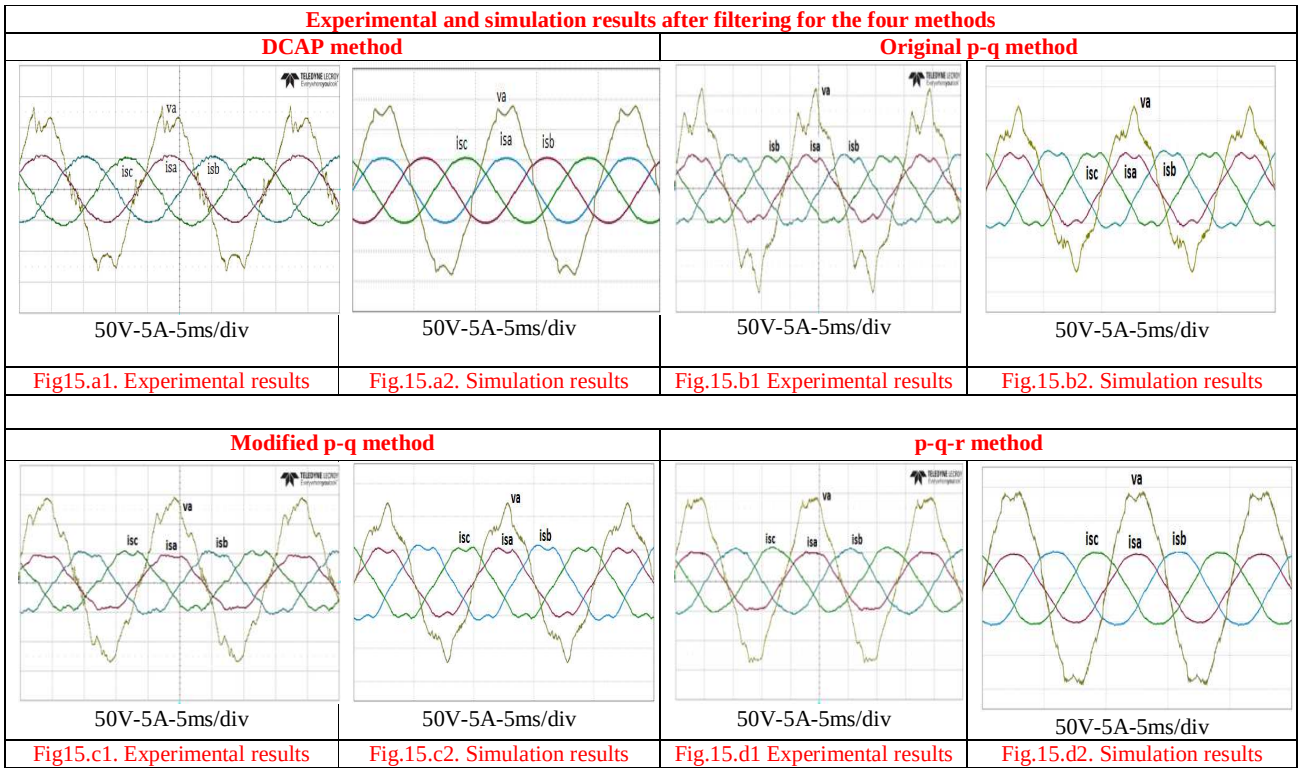

Fig. 15. System of currents at the source referenced to the voltage v_a of the phase a.

Table.4. Comparison of current THD and RMS values for all methods after filtering

Method		Experimental Source currents			Simulation Source currents		
		i_a	i_b	i_c	i_a	i_b	i_c
DCAP	THD_i %	3.2	3.3	3.9	2.8	2.7	3
	RMS (A)	3.83	3.77	3.79	3.78	3.78	3.78
Original p-q	THD_i %	7.8	8.4	8.3	7.8	8.1	8
	RMS (A)	3.61	3.9	3.7	3.62	3.95	3.8
Modified p-q	THD_i %	6.8	8.2	9.8	8	8	8
	RMS (A)	3.57	3.92	3.75	3.6	4	3.8
p-q-r	THD_i %	5.2	4.2	6.4	5	4.5	6.2
	RMS (A)	3.57	3.89	3.75	3.63	3.93	3.82

Results given by Fig.15 show that for the DCAP the currents system is sinusoidal despite the perturbation on voltages at the P_{cc} for both experimental Fig15.a1 and simulation Fig15.a2 results. For the p-q method Fig.15.b1 and Fig.15.b2 and for the modified p-q method Fig.15.c1 and Fig15.c2 currents are distorted after filtering. These two methods do not achieve sinusoidal currents

under perturbed voltages. For the p-q-r theory in Fig.15.d1 and Fig.15.d2, currents are better than those provided by the p-q and modified p-q but there are not sinusoidal. Table.4 gives numerical values for current THD and current RMS for each phase for both experimental and simulation results.

In term of currents system harmonic perturbation, Fige.16 gives the comparison between current *THD* for the three-phase and for the four methods and that shows that the DCAP method has the lower distortion on the three phases. It is better than all methods.

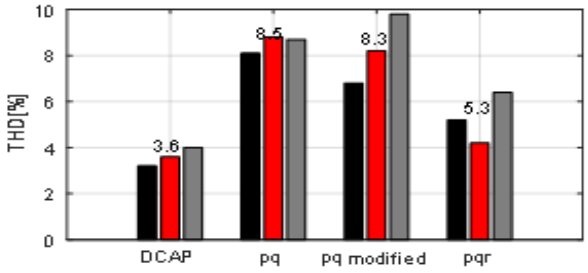

Fig.16 Comparison of performance for current THD

Regarding the balance of currents, the unbalance factor is measured according to EN 50160 with Fluke device and Fig.17 shows the unbalance diagram results after filtering for only the two methods DCAP in Fig.17.a and p-q-r in Fig.17.b. The value of the negative-sequence component is displayed and has as value of 0.8% for the DCAP method and 5.5% for the p-q-r method.

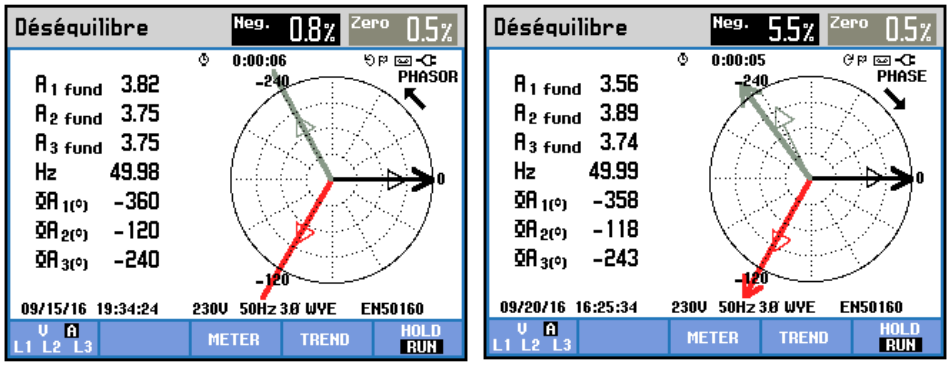

Fig.17.a) DCAP method

Fig.17.b) p-q-r Method

Fig.17. Unbalance diagrams for DCAP and p-q-r after filtering

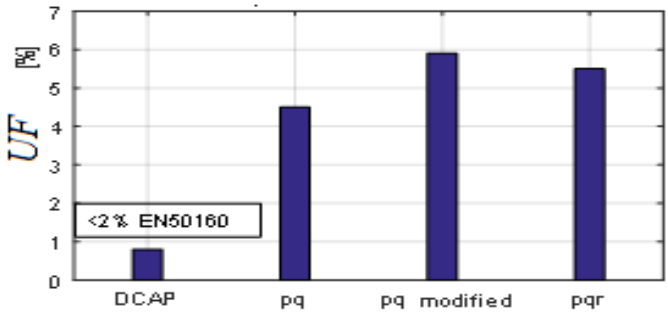

Fig. 18 Comparison of performance for Unbalance Factor

A comparison of performances regarding the unbalance factor $UF\%$ in Fig.18 is performed for all studied methods. It is shown that only the DCAP meet with standards recommendation with an $UF < 2\%$.

A summary of performances for the studied methods is presented on Tab.5

Table.5 Summary of performances for all methods based on experimental results

Method	***Sinusoidal current or low THD***	***THD_i % (Average)***	***Balance of currents system according to international standard***	***UF %***
DCAP	*Yes*	*3.5*	*Yes*	*0.8*
Original p-q	*No*	*8.2*	*No*	*4.5*
Modified p-q	*No*	*8.3*	*No*	*5.9*
p-q-r	*Medium*	*5.3*	*No*	*5.5*

5. Conclusion

In this work we have presented a new control method for active filter application taking into account distorted and unbalanced supply voltages. This method is based on a new definition of desired active current in the source formulated as function of the active power and the fundamental voltages. We have showing that in the presence of a highly disturbed and unbalanced network, the standard methods such as the p-q method, the modified p-q method and the p-q-r can not perform a sinusoidal current at the source side and do not make it possible to satisfy the constraints dictated by the standard. The proposed DCAP method, object of patent application, can provides sinusoidal currents on the source side and an $UF < 2\%$ that meet with the international standard in addition to the lowest THD of current compared to the standard methods . The model of the proposed control strategy is validate by simulation and experimental work and these performances are compared to three other methods by the way of simulation and experimentation. It is shown the superiority of the DCAP strategy over the existing standard ones. This general method can be deployed on single-phase or multiphase systems with 3 or 4 wires. It's easy to implement and does not require PLL. We believe that it can provide solutions in the case of isolated or embedded systems.

ACKNOWLEDGEMENTS

This work has been supported by the PHC CEDRE 2016 project N°30108XK and the Lebanese National Council for Scientific Research (CNRS-L). The authors also gratefully thank the Research Council of Saint-Joseph University of Beirut, Lebanon, the laboratory LAPLACE, the Agence Universitaire de la Francophonie (AUF), the Institut Français of the French Embassy in Lebanon, and the Institut Supérieur des Sciences Appliquées et Economiques (ISSAE-CNAM Liban) for their financial contribution.

REFERENCES

[1] McBee, K.D.; Simoes, M.G., "Evaluating the long-term impact of a continuously increasing harmonic load demand on feeder level voltage distortion," Industry Applications Society Annual Meeting (IAS), 2012 IEEE, vol., no., pp.1,8, 7-11 Oct. 2012

[2] M. Masoum, P. S. Moses and A. S. Masoum, "Derating of Asymmetric Three-Phase Transformers Serving Unbalanced Nonlinear Loads", IEEE Trans. Power Delivery, vol.23, No. 4, Oct. 2008, pp. 2033-2041.

[3] IEEE Recommended Practice and Requirement for Harmonic Control in Electrical Power systems. IEEE St d.519-1992.

[4] K. J. Lee *et al*., "A novel active power filter for selective harmonic suppression based on a robust PLL Algorithm," *2012 3rd IEEE International Symposium on Power Electronics for Distributed Generation Systems (PEDG)*, Aalborg, 2012, pp. 416-422

[5] K. Arulkumar, D. Vijayakumar and K. Palanisamy, "Investigation of PLL performance for utility connected systems under abnormal grid conditions," *2016 IEEE International Conference on Power and Energy (PECon)*, Melaka, 2016, pp. 84-88.

[6] Tadjer Sid Ahmed, Habi Idir, Angel Scipioni," Direct Components Extraction of Voltage in Photovoltaic Active Filter Connected in a Perturbed Electrical Network (Based On Robust PLL Algorithm)" Energy Procedia, Elsevier. Volume 74, August 2015, Pages 966-972

[7] G. Wang and G. Zhang, "Direct AC main current control of shunt active power filters — Feasibility and performance," 2006 37th IEEE Power Electronics Specialists Conference, Jeju, 2006, pp. 1-6.

[8] M. Fajardo, J. Viola, J. Restrepo, F. Quizhpi and J. Aller, "Two-phase active power filter direct current control with capacitor voltages estimation and balance," 2015 IEEE Workshop on Power Electronics and Power Quality Applications (PEPQA), Bogota, 2015, pp. 1-6.

[9] A. Fereidouni and M. A. S. Masoum, "Enhancing performance of active power filter with fuzzy logic controller using adaptive hysteresis direct current control," 2014 Australasian Universities Power Engineering Conference (AUPEC), Perth, WA, 2014, pp. 1-6.

[10] M. Y. Artemenko, L. M. Batrak and M. A. A. Taher, "Combined control system with direct current formation for three-phase four-wire network shunt active power filter," 2014 IEEE 34th International Scientific Conference on Electronics and Nanotechnology (ELNANO), Kyiv, 2014, pp. 438-441.

[11] R. K. Patjoshi and K. K. Mahapatra, "Performance comparison of direct and indirect current control techniques applied to a sliding mode based shunt active power filter," 2013 Annual IEEE India Conference (INDICON), Mumbai, 2013, pp. 1-5..

[12] Kaura and V. Blasko, "Operation of a phase locked loop system under distorted utility conditions," in *IEEE Transactions on Industry Applications*, vol. 33, no. 1, pp. 58-63, Jan/Feb 1997.

[13] A.F. Hanna Nohra, M. Fadel and H. Kanaan; Direct Control for Active Power in three-phase application on perturbed network. ELECTRIMACS 2017, 4 th -6 th July 2017, Toulouse, France

[14] A.F.Hanna Nohra, H. Kanaan, M. Fadel Procédé de commande d'un filtre actif parallèle pour réseaux perturbés et filtre actif associé. International Extension Patent 10 /10/ 2017 n° PCT/FR2017/052783

[15] W. M. Grady, M. J. Samotyj and A. H. Noyola, "Survey of active power line conditioning methodologies," in *IEEE Transactions on Power Delivery*, vol. 5, no. 3, pp. 1536-1542, Jul 1990

[16] B. Singh, K. Al-Haddad and A. Chandra, "A review of active filters for power quality improvement," in *IEEE Transactions on Industrial Electronics*, vol. 46, no. 5, pp. 960-971, Oct 1999

[17] H. Akagi, "The state-of-the-art of active filters for power conditioning," *2005 European Conference on Power Electronics and Applications*, Dresden, 2005, pp. 15 pp.-P.15.

[18] Akagi, H.; Kanazawa, Yoshihira; Nabae, A., "Instantaneous Reactive Power Compensators Comprising Switching Devices without Energy Storage Components," Industry Applications, IEEE Transactions on, vol.IA-20, no.3, pp. 625-630, May 1984.

[19] H. Akagi, A. Nabae and S. Atoh, "Control Strategy of Active Power Filters Using Multiple Voltage-Source PWM Converters," in *IEEE Transactions on Industry Applications*, vol. IA-22, no. 3, pp. 460-465, May 1986.

[20] Peng, F.-Z.; Akagi, H.; Nabae, A., "A study of active power filters using quad-series voltage-source PWM converters for harmonic compensation," Power Electronics, IEEE Transactions on , vol.5, no.1, pp.9,15, Jan 1990

[21] J. L. Afonso, M. J. S. Freitas and J. S. Martins, "p-q Theory power components calculations," *2003 IEEE International Symposium on Industrial Electronics (Cat. No.03TH8692)*, 2003, pp. 385-390 vol. 1

[22] G. Superti-Furga and G. Todeschini, "Discussion on Instantaneous p-q Strategies for Control of Active Filters," in *IEEE Transactions on Power Electronics*, vol. 23, no. 4, pp. 1945-1955, July 2008

[23] A.F. H. Nohra, M. Fadel and H. Y. Kanaan, "A novel instantaneous power based control method for a four-wire SAPF operating with highly perturbed mains voltages," *2016 IEEE International Conference on Industrial Technology (ICIT)*, Taipei, 2016, pp. 1236-1241

[24] Fang Zheng Peng; Ott, G.W., Jr.; Adams, D.J., "Harmonic and reactive power compensation based on the generalized instantaneous reactive power theory for three-phase four-wire systems," Power Electronics, IEEE Transactions on , vol.13, no.6, pp.1174,1181, Nov 1998.

[25] Akagi, H.; Ogasawara, S.; Hyosung Kim, "The theory of instantaneous power in three-phase four-wire systems: a comprehensive approach," Industry Applications Conference,1999. Thirty-Fourth IAS Annual Meeting. Conference Record of the 1999 IEEE , vol.1, no., pp.431,439 vol.1, 1999.

[26] Hyosung Kim; Akagi, H., "The instantaneous power theory on the rotating p-q-r reference frames," Power Electronics and Drive Systems, 1999.PEDS '99. Proceedings of the IEEE 1999 International Conference on , vol.1, no., pp.422,427 vol.1, 1999

[27] Hyosung Kim; Blaabjerg, F.; Bak-Jensen, B.; Jaeho Choi, "Instantaneous power compensation in three-phase systems by using p-q-r theory," Power Electronics, IEEE Transactions on , vol.17, no.5, pp.701,710, Sep 2002

[28] Herrera, R.S.; Salmeron, P.; Hyosung Kim, "Instantaneous Reactive Power Theory Applied to Active Power Filter Compensation: Different Approaches, Assessment, and Experimental Results," Industrial Electronics, IEEE Transactions on , vol.55, no.1, pp.184,196, Jan. 2008

[29] Mehmet Ucar, Engin Ozdemir Control of a 3-phase 4leg active power filter under nonideal mains voltage condition Electric Power Systems Research, Volume 78, Issue 1, January 2008, Pages 58-73

[30] M. Aredes, H. Akagi, E. Hirokazu Watanabe, E. Vergara Salgado and L. FrizeraEncarnaÇÃo, "Comparisons Between the p--q and p--q--r Theories in Three-Phase Four-Wire Systems," in *IEEE Transactions on Power Electronics*, vol. 24, no. 4, pp. 924-933, April 2009

[31] I. Yuniantoro, R. Gunawan and R. Setiabudy, "The pqr-coordinate in the mapping matrices model of Kim-Akagi on power transformation based on Euler angle rotation method," *2013 International Conference on QiR*, Yogyakarta, 2013, pp. 121-126